

PATTERNS IN GROWTH¹

Ulf Grenander

April, 2004

VERY PRELIMINARY!

1 In the footsteps of d’Arcy Thompson

In the year 1917 an event occurred that must have seemed like a watershed to the small community of biologists that believed that mathematics had the potential to become a useful tool in their discipline. In that year d’Arcy Wentworth Thompson published his pioneering work "Growth and Form" in which he attempted to explain biological (and other) patterns by appealing to mathematical principles. In particular he argued, in the last chapter of the book, that transformations of coordinates could make clear how the resemblance of structures were expressed in a striking and often convincing manner.

He based his arguments on the dictum that "the search for differences or fundamental contrasts between the phenomena of organic and inorganic, of animate and inanimate things, has occupied many mens minds, while the search for commonality of principle or essential similarities, has been pursued by few; the contrasts are apt to loom too large, great though they be" and that "in general, no organic forms exist, save as are in conformity with physical and mathematical laws".

"Growth and Form" was received with enthusiasm, at least among the openminded public, but, surprisingly, it was admired by many but emulated by few. Although his way of thinking can be traced back to antiquity, for example to Aristotle, and while related ideas were pursued after his death by other scholars, it is only recently that they have been studied and extended systematically by mainstream biologists. A representative list of such attempts can be found in Bonner ed. (1982).

Among mathematicians one finds even fewer researchers following d’Arcy Thompson until recently. The pathbreaking work by Bookstein beginning with his monograph appearing in 1978 and continuing forcefully in a huge stream of publications argued for using statistical ideas to elucidate problems of biological growth. The somewhat related work by Kendall ,see Kendall et al (1999) for an up to date presentation, was concentrated on the purely mathematical aspects but was also used in applications, among others archeology. Pattern theory as presented in Grenander (1993) and earlier emphasized the compositional and

¹This work has been supported by NSF DMS-00774276 and by ...

transformational properties of patterns of general form. This led to computational anatomy, see Grenander, Miller (1998) and in its most recent form in Beg, Miller, Trounev, Younes (2002). This is the starting point for the present study.

2 Invariances and coordinate systems

Consider an organism O , living in the background space $X = \mathbf{R}^3$ and developing as a function of time, $O = O(t)$. It is made up of disjoint components $O = \cup g^\alpha$ such that each generator (anatomical component) g^α is fairly homogeneous w.r.t. growth properties as controlled by the genetics; examples will be given later.

The organism grows as expressed by a composition semi-group $\Phi = \{\phi(s, t); -\infty < s < t < \infty\}$ of diffeomorphisms from $DIFFEO(X); X = \mathbf{R}^3$ so that

$$(i) \phi(t_1, t_2) \circ \phi(t_2, t_3) = \phi(t_1, t_3); t_1 < t_2 < t_3$$

$$(2) \phi(s, t) \text{ is continuous in } s, t \text{ (topology to be decided later)}$$

$$(3) \phi(t, t) = id(X).$$

The behavior of the mapping $x \rightarrow \phi(x)$ from a point $x \notin O(s)$ at time s is irrelevant. Growth will be represented as

$$O(t) = \phi^{-1}(t_0, t)O(t_0); t_0 \text{ fixed} \tag{1}$$

It will be assumed that the α -partition is invariant w.r.t. ϕ 's so that the genetic properties remain constant along trajectories induced by Φ .

Consider the Galilean space-time group

$$S = \{-\infty < t < \infty\} \times SE(3) \tag{2}$$

with elements generically denoted by s . The set of all growths $(t, \phi(\cdot, \cdot))$ invariant with respect to S is called a growth pattern². But we can also deal with other growth patterns, for example by replacing $SE(3)$ in (1) by $DIFFEO(X)$.

The space-time coordinate system $\{-\infty < t < \infty\} \times X$ is *absolute* in contrast to the *biological coordinate system* that we shall use:

$$\{0 < \tau < \infty\} \times \Xi \tag{3}$$

meaning that we measure time for O from its birth $\tau = 0$ and location on $O(\tau)$ by the value ξ of x at time 0 where we use Lagrangian coordinates and consider the trajectories in absolute

²see Grenander (1993) for pattern theoretic terminology

space to be denoted by $x(\tau) = \phi(t_0, \tau)\xi$, where ξ enumerates the trajectories with the initial values $x(\xi, 0) = \xi \in \Xi$. Since we are dealing with diffeomorphisms the function $x = x(\xi, \tau)$ has a well defined inverse $\xi = \xi(x, \tau)$.

REMARK. We add in passing that we may have concentrated too much on diffeomorphic mappings. Many biological processes exhibit destruction of topology, say in pathological growth and decay. Better keep this in mind for future use.

For short time intervals (s, t) it may happen that Φ is time invariant so that we can write with some abuse of notation $\phi(s, t) = \phi(t - s)$. Anyway, we shall often write $\phi(t)$ instead of $\phi(t_0, t)$.

3 Properties of the deformations

With standard notation

$$\dot{f} = \frac{\partial}{\partial t} f \text{ for fixed } \xi \quad (4)$$

$$f_t = \frac{\partial}{\partial t} f \text{ for fixed } x \quad (5)$$

we can write $v = \dot{\phi}$ and introduce the deformation gradient as the Jacobian $F = \frac{\partial(\phi)}{\partial(\xi)}$ taking 3×3 matrices as values. If the map $\phi : \Xi \rightarrow X$ is diffeomorphic with an inverse $\Phi : X \rightarrow \Xi$ we also get the inverse $G = \frac{\partial(\Phi)}{\partial(x)}$, $G = F^{-1}$.

We also consider the Jacobian matrix

$$J = \frac{\partial(v)}{\partial(x)} = \begin{pmatrix} \frac{\partial v_1}{\partial x_1} & \frac{\partial v_1}{\partial x_2} & \frac{\partial v_1}{\partial x_3} \\ \frac{\partial v_2}{\partial x_1} & \frac{\partial v_2}{\partial x_2} & \frac{\partial v_2}{\partial x_3} \\ \frac{\partial v_3}{\partial x_1} & \frac{\partial v_3}{\partial x_2} & \frac{\partial v_3}{\partial x_3} \end{pmatrix} \quad (6)$$

and write it in the polar decomposition $J = PO$ where P is a non-negative definite matrix and O is an orthogonal matrix. Let P have the eigen-values $\lambda_1, \lambda_2, \lambda_3$ and classify the deformation qualitatively at (t, x) as

- 1) *proper growth* if $\lambda_1 > 1, \lambda_2 >, \lambda_3 > 1$
- 2) *proper decay* if $\lambda_1 < 1, \lambda_2 < 1, \lambda_3 < 1$
- 3) else: *mixed growth*

The amount of deformation can be numerically expressed by $\det(J) = \lambda_1 \lambda_2 \lambda_3$ or by $\text{div}(v) = \lambda_1 + \lambda_2 + \lambda_3 - 3$,

4 Data source

So far the discussion has been too general. From now on we shall assume that data have been obtained in the following way. Mice from a genetically homogeneous strain are studied using MR observations of their brains under a period of time $T = [0, \tau_n]$ at times $\tau_1 < \tau_2 < \dots < \tau_n$. The output of the magnetic resonance camera at these times will be real valued arrays $I^{\mathcal{D}}(i); i = 1, 2, \dots, n$ of size $l_1 \times l_2 \times l_n$ corresponding to a rectangular region of size L_1, L_2, L_3 in X .

Now we repeat this with mice from another genetically modified strain and compute the diffeomorphic mappings (see the next section) from one time to the next one. We get a scheme like the one in Figure 1 where we have used m genotypes and 3 replications per

genotype.

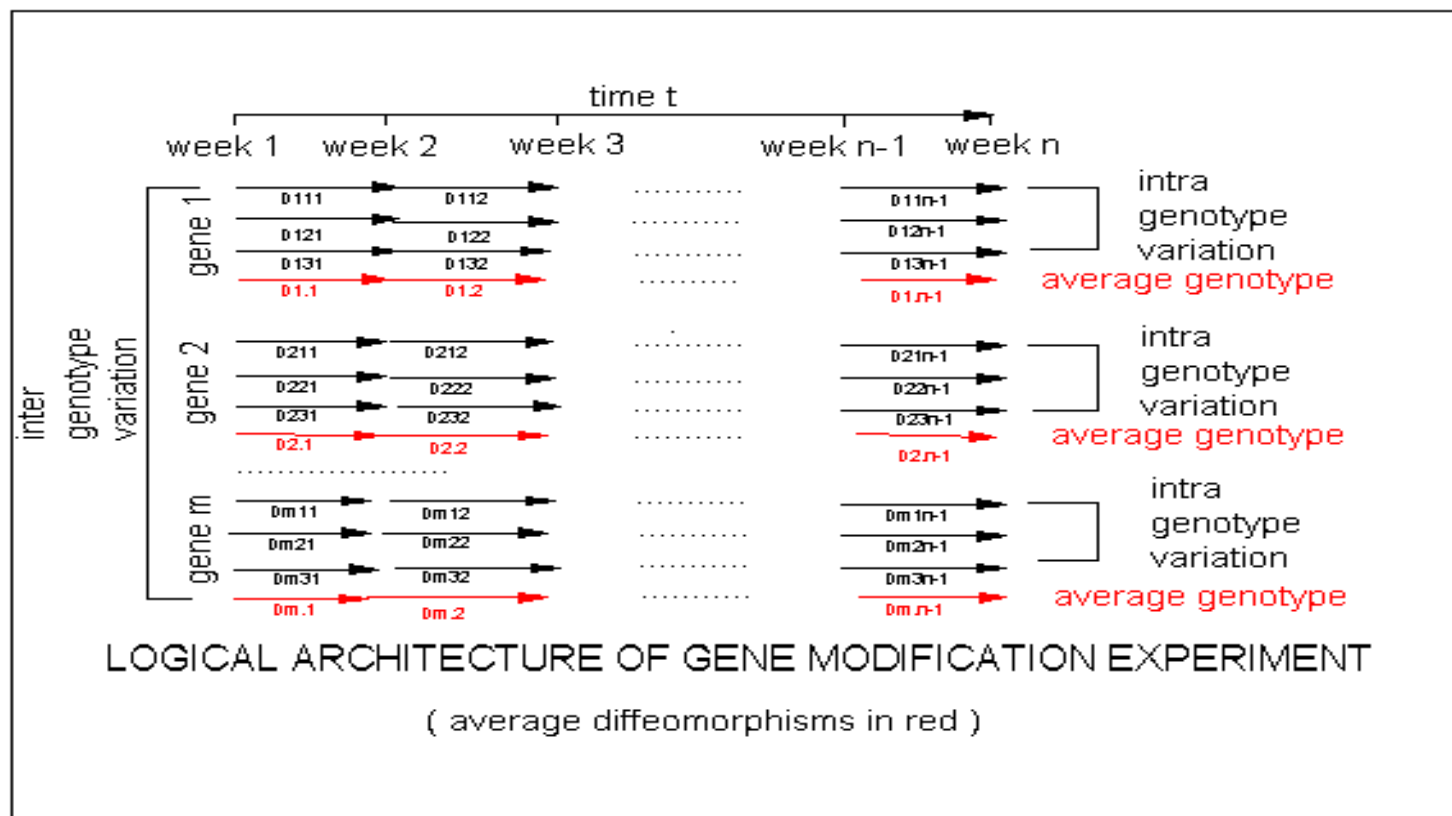


Figure 1

Let us classify data according to

- (i) genetic setup γ ; $\gamma = 1$ meaning unmodified gene; $\gamma = 2$ meaning knockout gene.
- (ii) organism component α enumerating the component used including the entire organism
- (iii) replication number $r = 1, 2, \dots, m$ for the different mice used in the data set with γ, α fixed.
- (iv) duration t for age $t = 1, 2, \dots, T$ weeks

This defines the the subsets $DATA(\gamma, \alpha, i, t)$, for example $DATA(1, 3, :, 5) \subset DIFFEO(X)$ meaning all the diffeomorphisms observed for unmodified gene, anatomical component 3, all mice in the class, age 5-6 weeks.

5 Estimating the deformations

When we have obtained the camera output I^D we try to represent it as a deformation of a template I_{temp} via a mapping $\phi : X \rightarrow X$. This can be done in many ways and we shall mention a few. They have in common that they are obtained by minimizing some energy.

5.1 Elastic deformations

Using an elasticity analog one can use the energy (one of many similar alternatives)

$$E(\phi) = \int_X [I^D(x) - (\phi^{-1}I_{temp})(x)]^2 dx + \int_X (L\phi)^2(x) dx \quad (7)$$

where L is a differential operator that measures smoothness. This is easy to implement, but has the drawback that the resulting mapping $\phi = \text{minarg} E(\phi)$ is not always diffeomorphic; see Christiansen (1994). This is true in particular for large deformations, when the Jacobian determinant can become zero or negative. For small deformations the diffeomorphic property will often hold.

SUGGESTION: *One way to remedy this may be to add a penalty term $\text{const} \times \int_X \log \det(J) dx$ to the right hand side of (7), but we do not know if this really is successful.*

5.2 Group cascade deformations

Another way to avoid singular behavior is to use a group cascade $\mathcal{C} = (S_1, S_2, S_3, \dots, S_n)$ with associated prior probability measure $\mathcal{P} = (P_1, P_2, P_3, \dots, P_n)$; see Matejic (1997) For example

$$\begin{aligned} S_1 &= \text{TRANSLATION}(X) \\ S_2 &= \text{SE}(3) \end{aligned}$$

$S_3 = \text{SA}(3)$
 $S_4 = \text{BENDING}(X)$
 $S_5 = \text{TORSION}(X)$
 \dots
 $S_n = \text{DIFFEO}(X)$

Then we apply the construction in the previous section using S_1 as the similarity group which transforms $I^{\mathcal{D}}$ into I_{temp}^1 via some transformation ϕ^1 . Then, using I_{temp}^1 as the new template the procedure gives a new I_{temp}^2 via a transformation ϕ^2 and so on. The first transformations are low-dimensional and diffeomorphic. The last (small) deformations are likely to be diffeomorphic and then the composition transformation $\phi = \phi^n \circ \phi^{n-1} \circ \dots \circ \phi^1$ will then also be diffeomorphic.

5.3 Flow deformations

Instead of using the analogy with elasticity theory one can appeal to fluid dynamics to supply the transformations. One variation of this idea generates diffeomorphic flows from a velocity field $v(\cdot)$ forced to be smooth enough; see Beg, Miller, Trounev, Younes (2002). The flow will be the solution of the variational problem

$$\text{argmin}_v \left\{ \int_0^1 \|v\|_{Sobolev}^2 dt + \|\phi^{-1} \circ I_{temp} - I^{\mathcal{D}}\|_2^2 \right\} \quad (8)$$

where $\|\dots\|_{Sobolev}$ is an appropriate Sobolev norm and the flow is given as the solution of the differential equation

$$\frac{dv}{dt} = \phi(v); \phi = id \text{ for } t = 0 \quad (9)$$

This method requires more computing power, but is guaranteed to lead to diffeomorphic mappings. It is vaguely related to the group cascade approach but it deforms the template continuously, rather than stepwise.

Another variation uses the same energy formulation augmented by a term penalizing the misfit of template landmarks $x_k^{template}$; $k = 1, 2, \dots, K$ to observed landmarks $x_k^{\mathcal{D}}$; $k = 1, 2, \dots, K$

$$\sum_{k,l=1}^K (x_k^{temp} - x_k^{\mathcal{D}}) \Sigma^{-1} (x_l^{temp} - x_l^{\mathcal{D}})^T \quad (10)$$

with some positive definite matrix Σ . Fitting the landmarks will produce a closer fit to the observed image $I^{\mathcal{D}}$ but has the side effect of producing nearly singular behavior in the neighborhood of the landmarks. This implies that when differential operators are applied

to the mapping artifacts will appear. They will have no biological significance and can invalidate the following statistical analysis. It can look like Figure 2

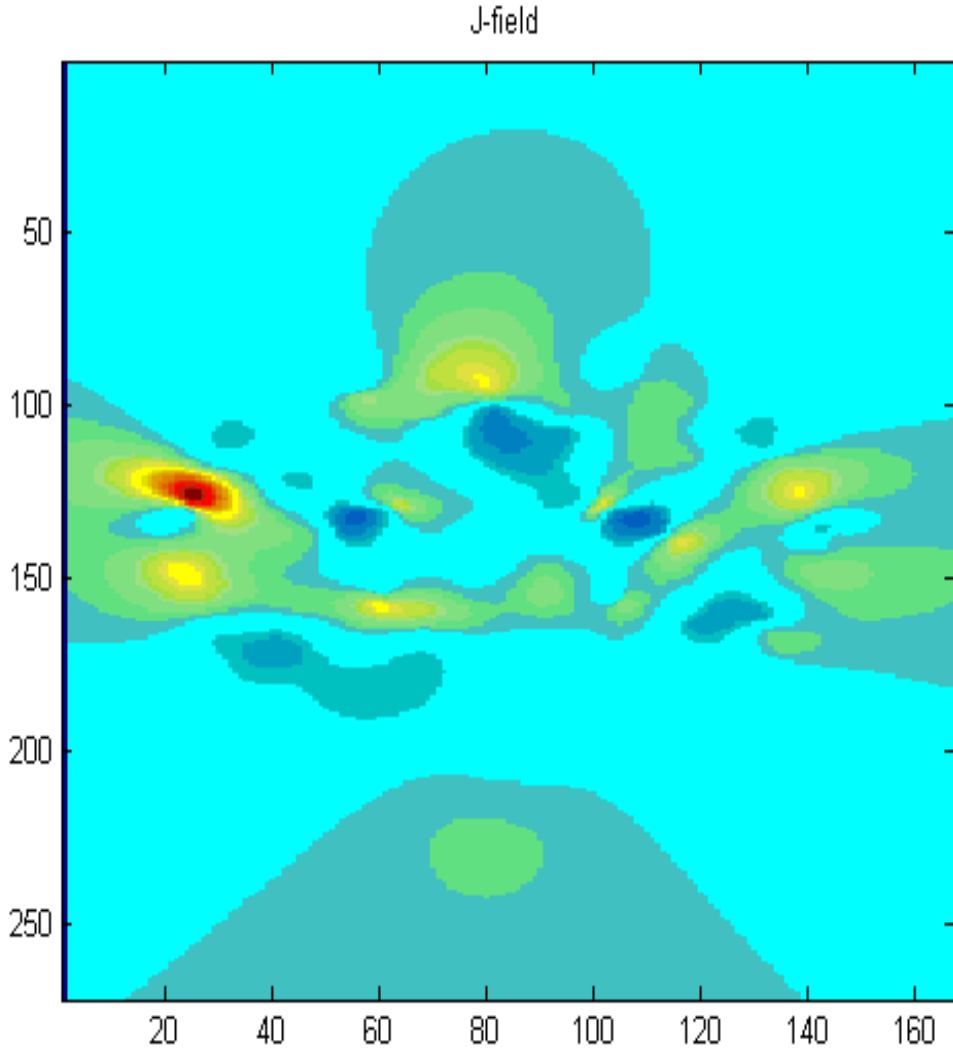


Figure 2

and sometimes even worse. If we want to drive the inference using only the observed image I^D we may achieve better fit as follows.

SUGGESTION: *Augment the energy expression in (7) with the term*

$$\int_X \left\| \phi^{-1} \circ \frac{dI_{temp}(x)}{dx} - \frac{dI^D(x)}{dx} \right\|^2 dx \quad (11)$$

so that the inference takes advantage of where the big values of the gradients template/observation are located.

5.4 Allometric growth

The above methods of determining the mappings $I_{temp} \rightarrow I^*$, where I^* is an approximation of I^D may be useful, at least after modification, for studying growth. However, biological growth is often *allometric*: different parts of the organism may grow at different rates as controlled by the genetic set up of the various parts. This is not accounted for by the schemes described in sections 5.1 - 5.3. When the emphasis is on differential growth rates, as in our present study, we must incorporate genetic differences in the growth model. We shall present two ways of doing this, both quite incomplete, but the second one seems to be biologically more meaningful than the first which is based on fluid mechanics analogies.

6 Representing growth

The first attempt still relies on mechanical analogs to the dynamics of fluids and has little biological basis. The other one is built on ideas of local growth and cell arrangements/movements/transformations; it seems closer to biological reality but introduces new mathematical difficulties.

6.1 Genetics preserving flows

Returning to the above discussion let us remind the reader of some earlier comments. We are again confronted with the question of choosing an intrinsic coordinate system. Although equations of motions are usually simpler in Eulerian formulations, here we will have equations with Lagrangian components relating to the cells along the trajectory. The growth tendency should be expressed in such Lagrangian coordinates. This will lead to some unavoidable mathematical complications, but we believe that we will be able to cope with them.

More concretely, let the trajectories in absolute space be denoted by $x(t) = \phi(\xi, t)$ where ξ enumerates the trajectories with the initial values $x(\xi, 0) = \xi \in \Xi$. We could start with the PDE for incompressible Navier-Stokes,

$$SPDE : \frac{Dv}{Dt} = -grad p + \mu\Delta v \tag{12}$$

but with the *growth pressure* p being a given function of ξ , not of x , and with a parameter μ that plays a role similar to that of viscosity for fluids. For example, cells belonging to the hippocampus may have different values for the pressure $p(\cdot)$ than cells in the frontal cortex due to genetic control. The gradient of $p(\cdot)$ drives the organism to expand or contract

according to the genetic information stored in the cells. We will also have random terms representing biological variability, but that will be discussed later. The term Δv and the viscosity μ are introduced to ensure enough smoothness for the case to be studied later on when we also have random forces acting on the cell growth.

This model will not be adequate for describing growth processes since the assumed incompressibility contradicts growth. It will therefore be modified and we shall try the following. Note also the discussion in Mumford (2002), section 4.3, in terms of geodesics in homogeneous spaces.

We can write the momentum equation concisely as

$$(v_i)_t = \sum_{j=1}^3 \frac{\partial T_{ij}}{\partial x_j} \quad (13)$$

with the Cauchy stress matrix

$$T_{ij} = \mu \frac{\partial v_i}{\partial x_j} - p(\xi) \delta_{ij} \quad (14)$$

Following a suggestion by Constantine Dafermos we will proceed as follows. Start from the form of the momentum equation

$$(v_i)_t + \sum_{j=1}^3 \frac{\partial v_i v_j}{\partial x_j} = \sum_{j=1}^3 \frac{\partial T_{i,j}}{\partial x_j} + \text{randomness} \quad (15)$$

and the mass equation

$$\rho_t + \sum_{j=1}^3 \frac{\partial(\rho v_i v_j)}{\partial x_j} = 0 \quad (16)$$

and reduce expressions with derivatives w.r.t. x 's to expressions involving derivatives w.r.t. ξ 's using the Jacobian matrices F and G . This leads to the following system of stochastic PDE's

$$\dot{G}_{\beta j} = - \sum_{i,\alpha=1}^3 G_{\beta,i} \frac{\partial v_i}{\partial \xi_\alpha} G_{\alpha,j} \quad (17)$$

$$\dot{v}_i = \sum_{\alpha=1}^3 \frac{\partial S_{i,\alpha}}{\partial \xi_\alpha} + n_i \quad (18)$$

where we have introduced the matrix-valued function S with components

$$S_{i,\alpha} = \frac{1}{\det(G)} \left[\mu \sum_{\beta,j=1}^3 G_{\alpha,j} \frac{\partial v_i}{\partial \xi_\beta} G_{\beta,j} - p(\xi) G_{\alpha,i} \right] \quad (19)$$

and n_i is the random term corresponding to biological variability.

With vector-matrix notation one can write (17) and (18) as

$$\dot{G} = -\frac{\partial(v)}{\partial(\xi)}GG^T \tag{20}$$

and

$$\dot{v} = \frac{\partial S}{\partial \xi} + n \tag{21}$$

This system has 12 equations (9 in (19), 3 in (20)) and 12 unknown functions (3 components in the vector v and 9 components in the matrix G), note that $p(\cdot)$ is assumed to be known in advance. Equations (20) and (21) form our SPDE. We will probably use Neumann boundary conditions along the sides bounding the box X and initial values

$$v(\xi, 0) = 0, G(\xi, 0) = I \tag{22}$$

If this growth model turns out to be realistic we will be confronted by several questions:

1) In order to judge the performance of the model we should synthesize it applying it to some of the MRI's we already have. There does not seem to exist any software specialized for this set up, but it may be possible to use programs of general nature and specialize them to the case above. It appeared troubling that the currently available displacement fields seemed to have fairly chaotic divergence, but this was seen to be a computational artefact due to landmark constraints.

2) Using our existing data for template + image and already computed diffeomorphisms for the duration one week, how do we estimate the variation of $p(\cdot)$ over Ξ ? Perhaps we could use some simple time-averaging behavior, but a full ML solution would require a careful examination of the form of the likelihood function involving a Jacobian.

3) How would a minimum energy derivation of the solution be organized? Too early to say yet.

4) If we can handle 1) - 3) we can use the results in FANOVA .

6.2 Simulating the SPDE.

Waiting for 3D software to solve the SPDE we have developed MATLAB code for the 2D case. It uses a rough difference scheme for integrating the differential equation. We get for

example

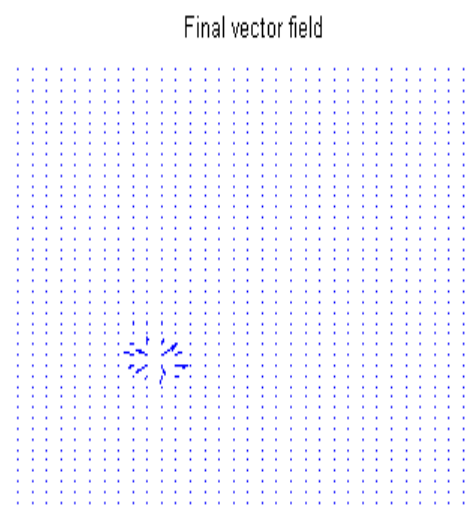
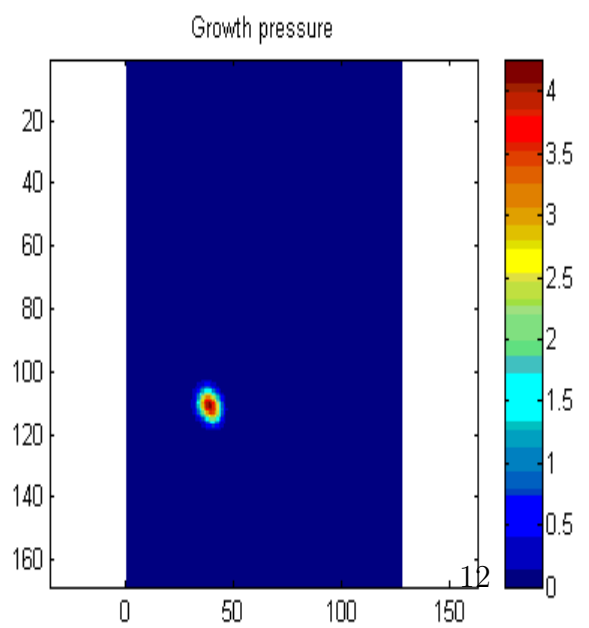
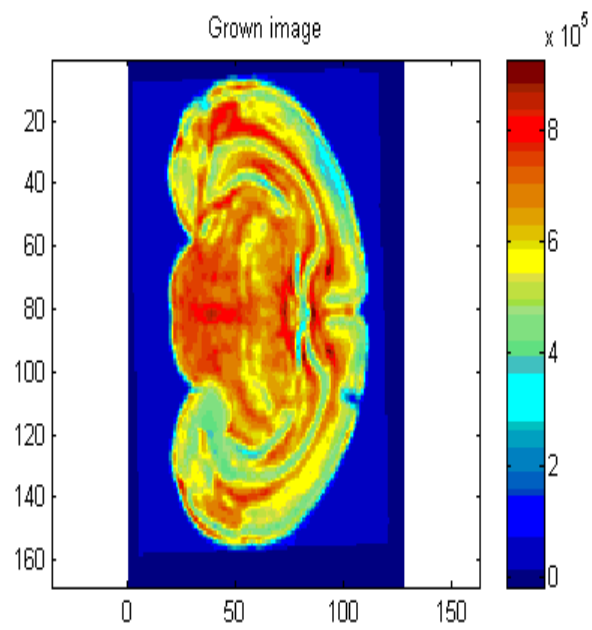
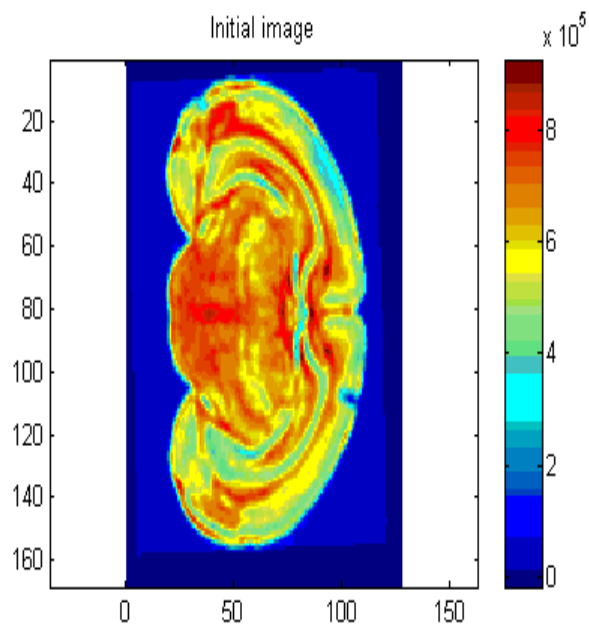


Figure 3

The structure at location $(45,125)$ in the upper left panel has grown as is seen in the upper right panel. The lower left panel shows the growth pressure and the right lower one presents the resulting displacement field.

In Figure 2 we see a growth area at $(45,80)$ and a decay area at $(80,80)$, resulting in the

structure in the right upper panel.

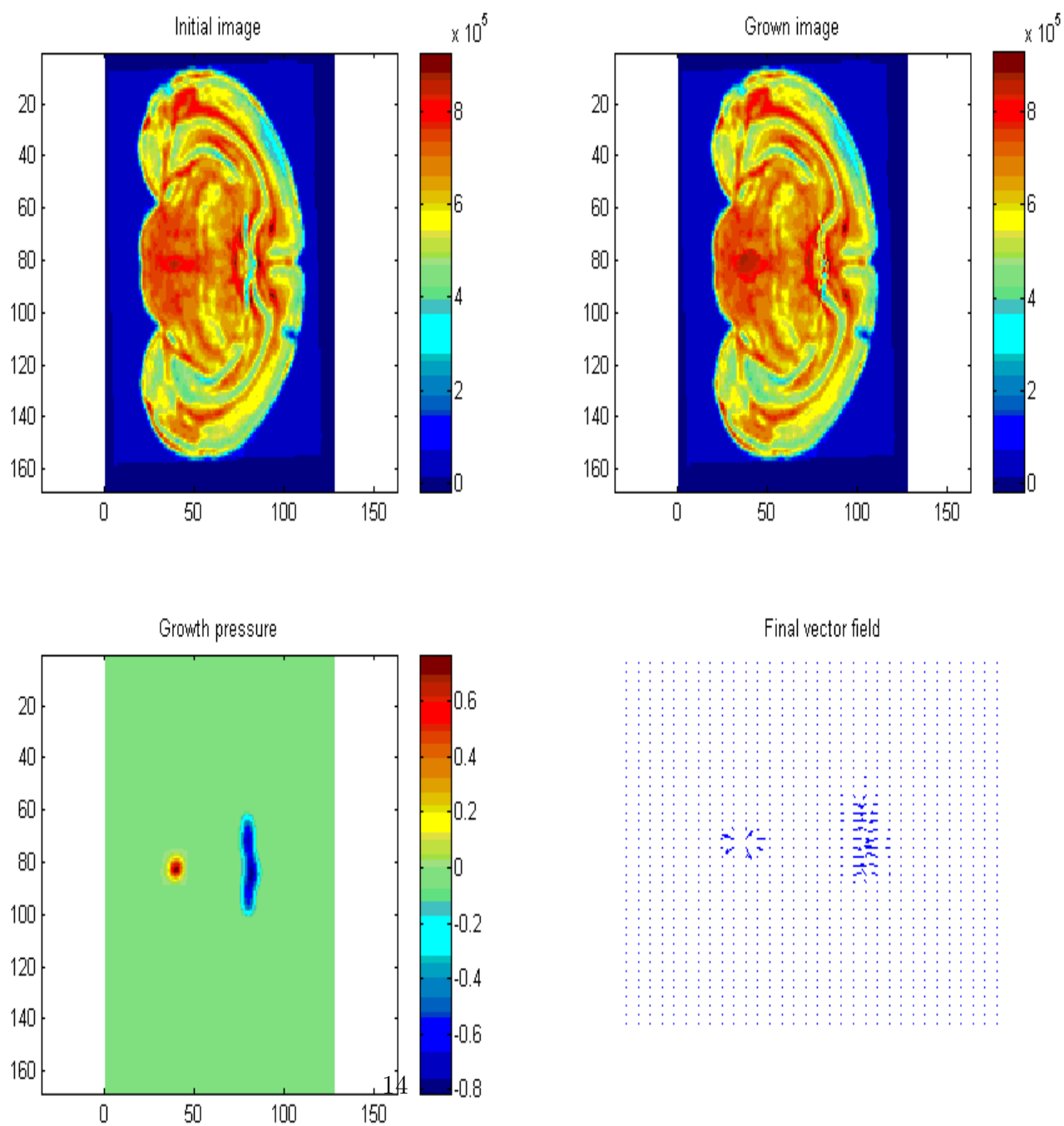


Figure 4

We have seen similar phenomena before, see Grenander, Miller (1998), but they were not based on a growth model as are Figures 3 and 4.

We mention parenthetically that if we leave out the viscosity term in (19) we get a simpler model, both analytically and computationally, but numerical experiments have convinced us that the growth then tends to be non-cohesive which contradicts experience. Therefore we have not pursued this alternative.

The SPDE has a regular solution for sufficiently small durations, but nothing guarantees that this holds for long durations. Indeed, the non-linear form of the flow can very well lead to shockwaves and other singularities. If shockwaves occur this may have interesting biological interpretations, but this remains to be seen.

The paradigm of fluid flows of images has served us well, but biological growth is different from mechanical flow, so that we ought to be open to non-mechanical models for growth, see Section 6.5.

6.3 How to estimate the growth pressure?

If it turns out that the SPDE is indeed useful for our purpose, the question arises how the $p(\cdot)$ -function can be estimated. We offer the following crude attempt that should be understood only as a first approximation.

If we neglect the viscosity term in (10) as well as the local variability of the deformation tensor G , we see that $\dot{v} \propto \text{grad } p$ where the degree of approximation is certainly in doubt. Integrating this approximate proportionality relation we get

$$v(\xi, 1) = \int_{t=0}^1 \dot{v}(\xi, t) dt \propto (\text{grad } p)(\xi) \quad (23)$$

Now recall that a vector field $F = \{f(x); x \in X\}$ can be expressed via Helmholtz' theorem as a sum

$$F = F_1 + F_2 = \text{grad}E + \text{curl}F \quad (24)$$

in terms of a scalar potential E and a vector potential F , so that the first term in the sum is irrotational, $\text{curl}F_1 = 0$, and the second term is solenoidal, $\text{div}F_2 = 0$. Apply div to both sides of (24)

$$\text{div}F = \text{div } \text{grad}E = \Delta E \quad (25)$$

It seems reasonable to state $E(x) = 0; x \in \partial X$ so that with these boundary conditions

$$E = \Delta^{-1} \text{div}F \quad (26)$$

since the operator Δ is invertible on the subspace of functions vanishing on ∂X . Hence the ratio, for example with L_2 norm,

$$r_{irroot} = \frac{\|V_1\|}{\|V\|} \quad (27)$$

expresses the degree to which the velocity field is irrotational. Apply (14) and (17) to data, using classical over relaxation to determine the inverse of the Laplacian Δ , we get the estimate of the growth pressure

$$p^*(\xi) = (\Delta^{-1}div v)(\xi, 1) \quad (28)$$

Look at the artificial growth data in Figure 5. The growth pressure is positive in the upper part of the organism (expansion) and negative in the lower part (compression) as is

seen in the upper right panel.

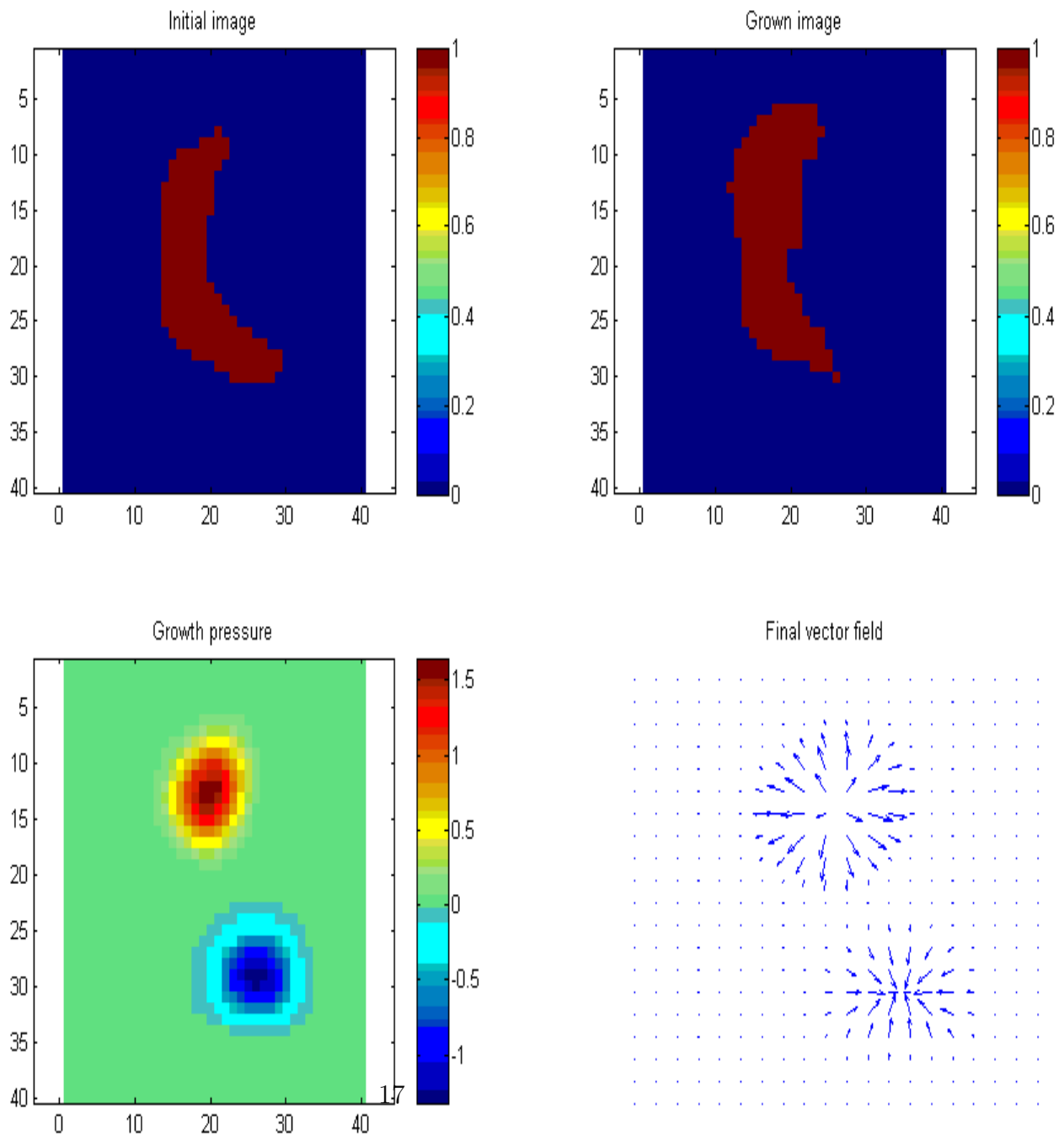


Figure 5

Compute the estimate in (28); the result is shown in the right panel of Figure 6. It does not look too bad, but we had better exercise caution keeping in mind that experimenting with artificial data often leads to misleadingly good result.

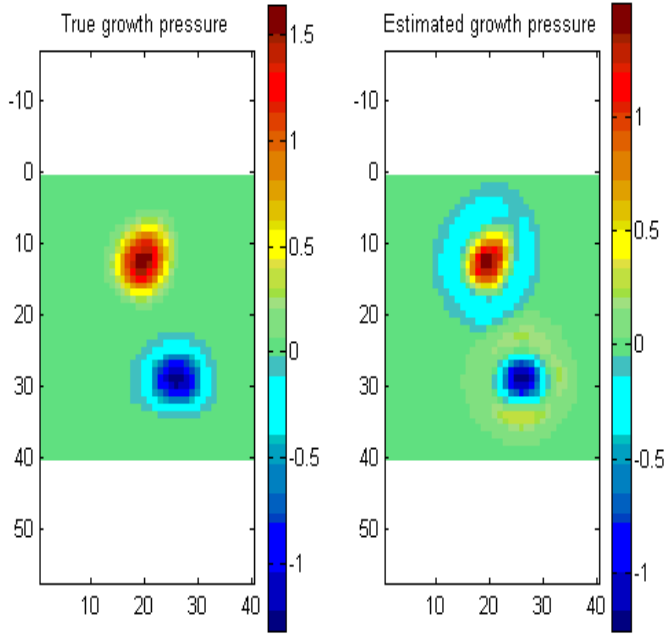


Figure 6

A more ambitious approach could be based on ML estimation, but it remains to be seen how this could be done.

6.4 Proper growth

The term "growth" implies increasing volumes unless it is otherwise qualified. However, in previous section we have actually allowed "negative growth", i.e. decay. Nevertheless our main interest is certainly in "positive", or "proper", growth.

But what do we mean precisely when we use this term? We shall use the following interpretation.

We shall say that the organism exhibits proper growth at (ξ, t) in biological space-time if

there are positive h and d such that

$$\|x(\xi_1, \tau) - x(\xi_2, \tau)\| < \|x(\xi_1, t) - x(\xi_2, t)\| \quad (29)$$

for all $\|\xi_1 - \xi\| < d, \|\xi_2 - \xi\| < d, 0 < \tau < h$. Note that the condition is expressed in biological, not absolute coordinates.

If (29) holds, put $\xi_1 = \xi + d_1; \xi_2 = \xi + d_2$ and

$$x(\xi_1, \tau) - x(\xi_2, \tau) = x(\xi_1, t) - x(\xi_2, t) + D_1 - D_2 \quad (30)$$

$$D_1 = x(\xi_1, \tau) - x(\xi_1, t); D_2 = x(\xi_2, \tau) - x(\xi_2, t) \quad (31)$$

For $\tau = t + \epsilon$, we have

$$\|x(\xi_1, \tau) - x(\xi_2, \tau)\|^2 = \|x(\xi_1, t) - x(\xi_2, t)\|^2 + 2 \langle x(\xi_1, t) - x(\xi_2, t), D_1 - D_2 \rangle + \quad (32)$$

+

$$O(\|D_1 - D_2\|^2) \quad (33)$$

But for small ϵ we have $D_1 \sim v(\xi_1, t)\epsilon$ and similarly for D_2 . Hence the double product term in (34) must be non-negative as $\epsilon \downarrow 0$, so that the inner product $\langle x(\xi_1, t) - x(\xi_2, t), D_1 - D_2 \rangle$ must be non-negative. But this can be written asymptotically in terms of the Jacobian matrices

$$x(\xi_1, t) - x(\xi_2, t) \sim \frac{\partial(x)}{\partial(\xi)}(d_1 - d_2) \quad (34)$$

and

$$D_1 - D_2 \sim [v(\xi_1, t) - v(\xi_2, t)](\tau - t) \sim \frac{\partial(v)}{\partial(\xi)}(d_1 - d_2)(\tau - t) \quad (35)$$

Hence we get the condition for proper growth in terms of an inner product, for all d_1, d_2 ,

$$\langle \frac{\partial(x)}{\partial(\xi)}(d_1 - d_2), \frac{\partial(v)}{\partial(\xi)}(d_1 - d_2) \rangle \geq 0 \quad (36)$$

or, in terms of the matrix P

$$P = F^T \frac{\partial(v)}{\partial(\xi)} \quad (37)$$

we see that for proper growth P must be non-negative definite.

6.5 Genetics preserving seed mechanisms

Consider a time dependent organism $O = O(t)$ observed via some acquisition technology and represented in pattern theoretic terms as

$$O(t) = \sigma[g_1(t), g_2(t), \dots, g_n(t)] \quad (38)$$

In (1) the generators, the anatomical components $g_i(t)$, are allowed to change with time, to grow or decay, while the overall topology of the organism, described by the connector graph σ , remains the same. In other, words, we shall here be dealing with automorphic deformations³, not allowing creation or annihilation of components, so that we shall be dealing with fairly mature organisms, not with their embryonic development.

For example, O may be the brain of a mouse observed via magnetic resonance diffusion tensor micro-imaging at times $t = 1, 2, 3, \dots$, with the time unit being a week and time is counted after birth. The generators could then be hippocampus, caudate putamen, corpus callosum..., and finally a residual volume that stands for the remainder of what is observed of O .

$$O(t) = \sigma[\textit{hippocampus}(t), \textit{caudate putamen}(t), \textit{corpus callosum}(t), \dots, \textit{residual}(t)] \quad (39)$$

To each generator g we associate a generator index $\alpha = \alpha(g) \in \mathbf{N}$; the generator index indicates the growth properties of a generator so that $\alpha[g(t)]$ remains constant over time. The set A of all such α 's is *the anatomy of the organism*. We reserve the largest α value, m , to mean the entire organism.

The α -sets are assumed to be fairly homogeneous w.r.t. their genetically controlled growth properties. If this is not the case for the standard anatomical components, some of which were mentioned above, then the α -sets have to be redefined.

Absolute space $X = \mathbf{R}^3$ will express the location of $O(t)$ in coordinates $x = (x_1, x_2, x_3) \in X$ using either manual methods, say based on a Talairach coordinate system, or automatic registration methods estimating the element of a low dimensional Lie group. More importantly, we shall use a biologically motivated curvilinear coordinate system Ξ evolving together with the development of $O(t)$ such that it maps the genetic constitution of $O(0)$. In other words the genetic information at time t and location $\xi(t) = (\xi_1(t), \xi_2(t), \xi_3(t)) \in \Xi$ should be the same as at time $t = 0$ and location $\xi(0) = (\xi_1(0), \xi_2(0), \xi_3(0)) \in \Xi$. Absolute and biological coordinates will be related by

$$f(\cdot, t) : \Xi \rightarrow X; x = f(\xi, t) \quad (40)$$

Since the g 's carry the genetic information we can also think of α as defined as a function on the biological coordinate system Ξ , $\alpha = \alpha(\xi)$, constant on the anatomical components as they evolve due to growth.

³see Grenander (1993), p. 505

An attempt to do this was made in Grenander (2003) using flow ideas from fluid dynamics. Now we shall present an alternative that is built on the idea that biological growth is made up of a large number of small growth elements, for example mitosis, cell growth and cell motion.

Consider for each point ξ_{seed} in biological space Ξ a family F of diffeomorphisms $s_{\xi_{seed}}^\alpha : \xi \mapsto s_{\xi_{seed}}^\alpha(\xi)$ for all $\alpha \in A$. Let us close the set of all such mappings *algebraically w.r.t. function composition* so that we get the general form of the closure as

$$\{s_n \circ s_{n-1} \circ \dots \circ s_1\} \in [F] \quad (41)$$

We then close $[A]$ topologically (the topology to be specified later) and get the topological group $S = \overline{[F]}$. The elements of S are all diffeomorphic mappings $X \leftrightarrow X$. If F is large enough we will have $S = diffeo(X)$ but this need not be the case. Note that the relation in (41) means that *we are not dealing with linearity, multiplications by scalars and additions, but with function compositions.*

With some loss of generality let us assume all the s to be translation invariant so that

$$s_{\xi_{seed}}^\alpha(\xi) = s^\alpha(\xi - \xi_{seed}) \quad (42)$$

where the function $s^\alpha(\cdot)$ does not depend upon the seed ξ_{seed} . Growth caused by the seed ξ_{seed} will be given by the diffeomorphism in (3). Note that all the points x in absolute space have a biological coordinate $\xi(t)$ so that the ξ -coordinate system evolves in time representing growth. This growth model is a continuous version of one used in Grenander (1993), section 4.2.

To characterize the local properties of the s^α in 2D form the Jacobian matrix

$$J = \frac{\partial(s_1^\alpha, s_2^\alpha)}{\partial(\xi_1, \xi_2)} = \begin{pmatrix} \frac{\partial s_1^\alpha}{\partial \xi_1} & \frac{\partial s_1^\alpha}{\partial \xi_2} \\ \frac{\partial s_2^\alpha}{\partial \xi_1} & \frac{\partial s_2^\alpha}{\partial \xi_2} \end{pmatrix} \quad (43)$$

and write it in polar form as the product of a non-negative matrix P and an orthogonal O

$$J = PO = \begin{pmatrix} \lambda_1 & 0 \\ 0 & \lambda_2 \end{pmatrix} \begin{pmatrix} \cos \phi & \sin \phi \\ -\cos \phi & \sin \phi \end{pmatrix} \quad (44)$$

We can then separate cases

- 1) if $\lambda_1 > 1, \lambda_2 > 1$: *proper growth*
- 2) if $\lambda_1 < 1, \lambda_2 < 1$: *proper decay*
- 3) else: *mixed growth*

As a simple example of such diffeomorphisms we express the deformation in polar coordinates around the seed

$$\xi_1 = \xi_{seed}(1) + r \cos(\theta); \xi_2 = \xi_{seed}(2) + r \sin(\theta) \quad (45)$$

with

$$s^\alpha(\xi - \xi_{seed}) = (r_1 \cos(\theta), r_1 \sin(\theta)) \quad (46)$$

where the deformed radius r_1 is given by

$$r_1 = r/4 \text{ if } -4 < r < 4; r_1 = r - 3 \text{ if } r < -4; r_1 = r + 3 \text{ if } r > 4 \quad (47)$$

The function is graphed in Figure 1. Growth occurs in a circular region of radius 4 around the seed; other points are just pushed away by internal growth.

Now we iterate this by selecting seeds by a heterogeneous Poisson process with intensity λ_α for a generator g with $\alpha(g) = \alpha$, applying one diffeomorphism after another. The Poisson intensity is kept constant over α -sets in time for the short time intervals we have been considering. The resulting s -mappings is the stochastic growth controlled by the genetic setup (the α -values) of the different components of O .

The observant reader will have noticed that this is akin to the construction that d'Arcy Thompson used in his *Growth and Form*, see Thompson (1984), although the mathematics was not spelled out explicitly. He called it the *Method of Coordinates*, and we have indeed

emphasized the role of the coordiante system.

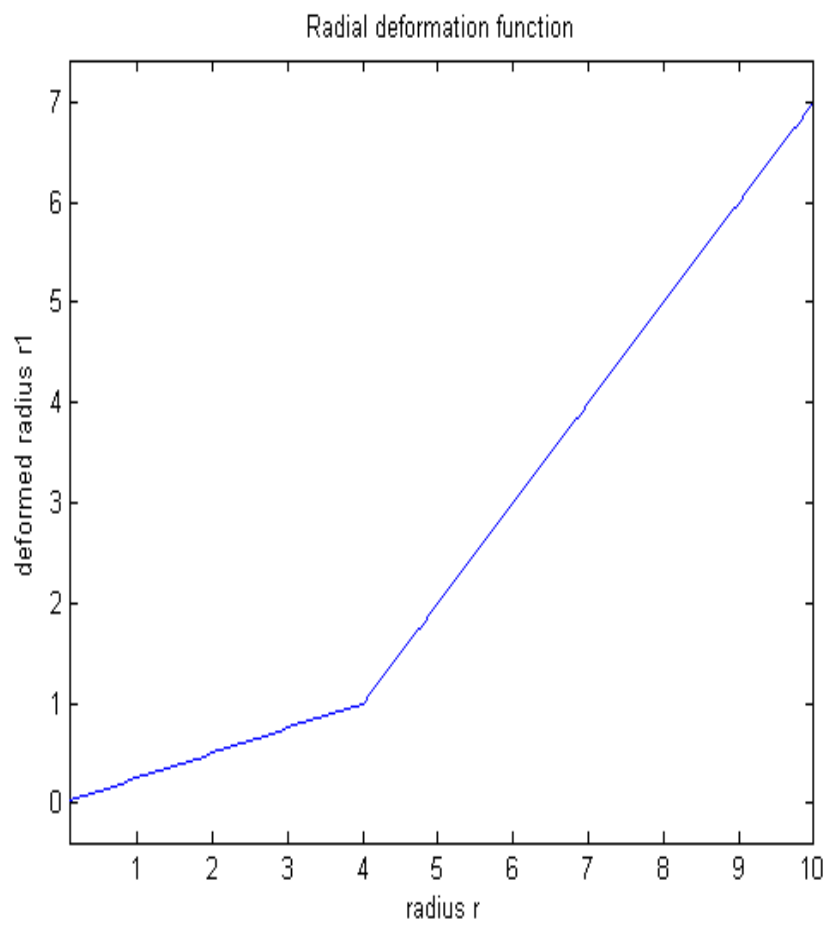


Figure 7

7 The evolving coordinate system.

To compute this growth model we discretize so that the biological coordinate system is given as the matrix pair

$$\Xi_1 = \{\xi_{1_1}, \xi_{1_2}; \nu_1 = 1, 2 \dots l_1, \nu_2 = 1, 2, \dots l_2\} \quad (48)$$

$$\Xi_2 = \{\xi_{2_1}, \xi_{2_2}; \nu_1 = 1, 2 \dots l_1, \nu_2 = 1, 2, \dots l_2\} \quad (49)$$

Of course the diffeomorphic concept does no longer apply in the discrete setting: when we invert the coordinates by solving the equations

$$\Xi_1(\xi_1, \xi_2) = x_1; \Xi_2(\xi_1, \xi_2) = x_2 \quad (50)$$

in the unknowns (ξ_1, ξ_2) for given (x_1, x_2) , it can happen that no solution exists or that there is more than one solution. Instead we search for a least squares solution that solves

$$\min[(\Xi_1(\xi_1, \xi_2) - x_1)^2 + (\Xi_2(\xi_1, \xi_2) - x_2)^2] \quad (51)$$

We illustrate this in Figure 8

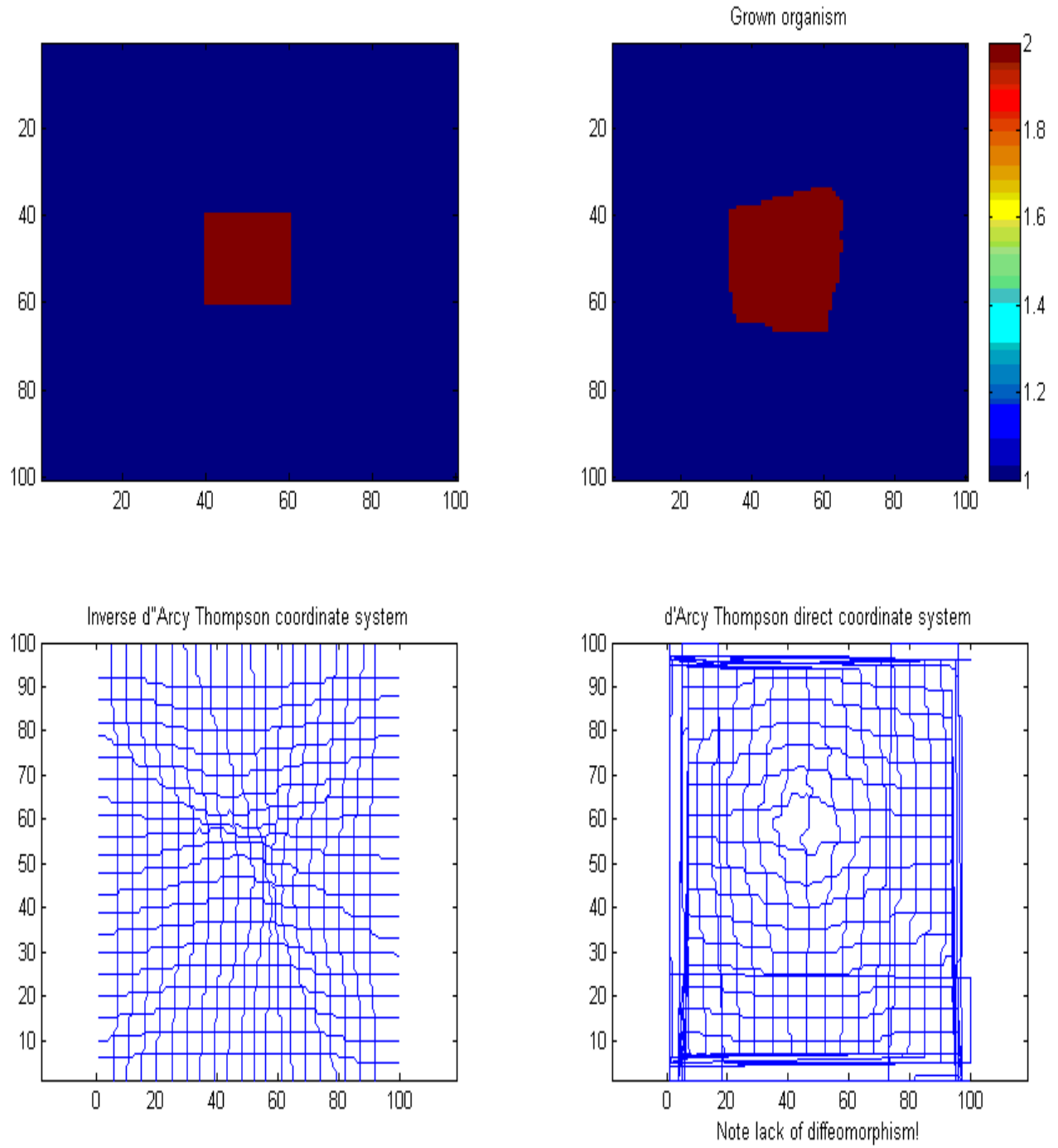


Figure 8

In the upper left panel there is the original organism, in the upper right the grown organism. The lower left panel displays Ξ_1, Ξ_2 , the d'Arcy Thompson coordinate, which shows how grown elements are selected from the inner ones, proper growth. The lower right one shows the solution to (51), the inverted d'Arcy Thompson coordinates, which shows how inner elements propagate outwards during the growth process.

For the sake of display we have chosen low λ_α values leading to a small number of iterations. It is clear, however, that in reality the small diffeomorphisms s_i should be iterated a large number of times corresponding to large Poisson intensities.

CONJECTURE: *Part I. The composition $s_n \circ \dots \circ s_2 \circ s_1$, suitably normalized, is asymptotically Gaussian on the diffeomorphic group.*

Part II. There is a law of large numbers on the diffeomorphic group

This could be organized in terms of a triangular array of random diffeomorphisms

ϕ_{11}

ϕ_{21}, ϕ_{22}

$\phi_{31}, \phi_{32}, \phi_{33}$

...

$\phi_{n1}, \phi_{n2}, \phi_{n3}, \dots, \phi_{nn}$

with probability measures $P_1, P_2, P_3, \dots, P_n$ attached to the 1st, 2nd, 3rd, ..., nth rows respectively. As $k \rightarrow \infty$ the P_k should contract around the identity $id \in DIFFEO(X)$ at a speed to be determined.

This problem has been studied in the 1D case where a surprising result, see Vitale (1974) and Grenander (1993), section 12.2, which raises doubt about Part I of the conjecture.

8 An example with both growth and decay.

To see how combined proper growth with decay is implemented by the random seed model, look at Figure 9.

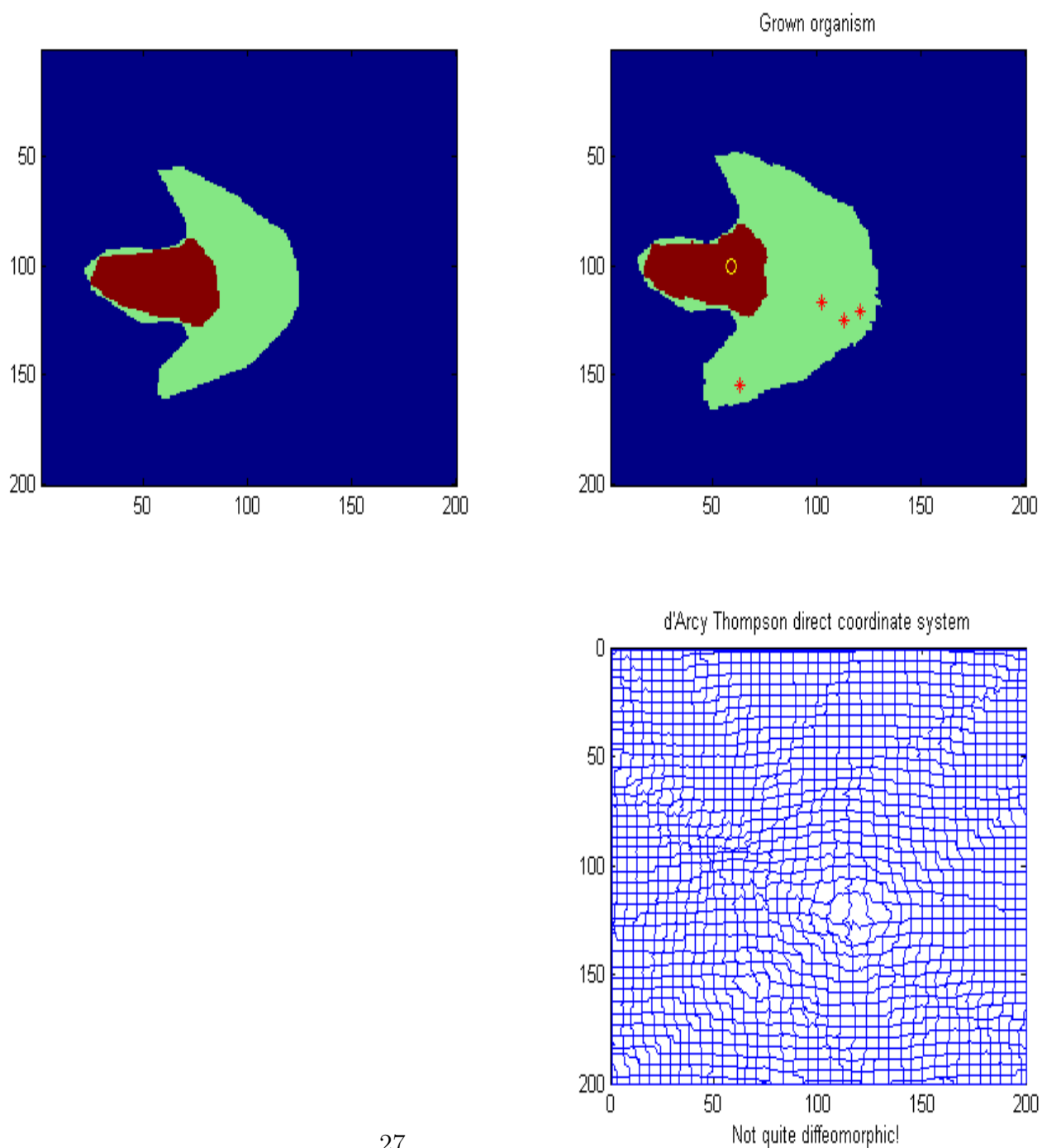


Figure 9

The organism consists of two parts, a large one in green with proper growth and a smaller in brown with slight decay. The upper right panel shows the result of growth/decay.

9 FANOVA of MRIs

Once we have access to estimated diffeomorphisms, perhaps using one of the methods discussed in section 5 we can proceed to their statistical analysis. We want to *discover differences in growth for different DATA sets*, for example between the diffeomorphisms

$$DATA(1, 3, :, 2) \text{ and } DATA(2, 3, :, 2) \quad (52)$$

representing the effect of gene modification in the growth of anatomical component 3 from age 2 weeks to 3 weeks. Or,

$$DATA(1, m, :, T) \text{ and } DATA(2, m, :, T) \quad (53)$$

representing the effect of gene modification in the growth of the whole organism from birth to maturity.

We would also like to construct tests of hypothesis that would measure the strength of the indicated effects. This resembles classical ANOVA, but with the difference that we are now dealing with high or infinite dimensional parameter and sample spaces (recall sieves), so that we are led to FANOVA; see the stimulating paper Antoniadis (2003).

9.1 Reduction of dimension

. To reduce the enormous dimensionality of the mappings we refer to the discussion of patterns in section 2 and shall approximate the ϕ 's by elements from the special affine group $SA(3)$ More precisely we shall use the 12 parameters of the group $x \rightarrow a + Bx$, three parameters in the vector a and 9 parameters in the non-singular matrix. The approximations a^*, B^* are simply given as solutions to

$$(a^*(\phi), B^*(\phi)) = \underset{x=(x_1, x_2, x_3) \in X}{\operatorname{argmin}} \quad \{[\phi_1(x) - a_1 - B_{11}x_1 - B_{12}x_2 - B_{13}x_3]^2 + \} \quad (54)$$

$$+[\phi_2(x) - a_2 - B_{21}x_1 - B_{22}x_2 - B_{23}x_3]^2 + [\phi_3(x) - a_3 - B_{31}x_1 - B_{32}x_2 - B_{33}x_3]^2 \} \quad (55)$$

Note the simplification in the estimation due to the fact that $SA(3)$ has the geometry of a vector space in contrast to, for example, $SE(3)$. On the other hand, it can be questioned

whether 12 degrees of freedom is enough to get a working approximation, or whether the $SA(3)$ need to be extended.

The relevant part of the estimate is B^* since the a^* -vector only means a translation that seems to have no biological meaning. Hence our reduced parameter has dimension 9.

9.2 Statistical test of hypotheses for genetic effects

If the estimates indicate the presence of a genetic effect on one or several anatomical components we could try to validate this by applying some statistical test. This would not be quite according to statistical orthodoxy but would correspond to common sense.

But trouble occurs when we perform the usual decomposition of quadratic forms in the ϕ 's followed by F-tests. Indeed, the distributions of numerator/denominator in the F-expression will not be the standard ones. This is caused by the strong spatial dependence between values taken by the diffeomorphisms. In spite of this it may be helpful during the data analysis stage to do the decomposition and study the behavior of the resulting averages and the quadratic forms, but not using them for a formal test of hypothesis.

Now we shall base the analysis on the lower dimensional parameter of the approximating $SA(3)$ group.

For data consisting of one sample $DATA(1, \alpha, i, t); i = 1, 2, \dots, n_1$ vs $DATA(2, \alpha, i, t); i = 1, 2, \dots, n_2$ leading to the diffeomorphisms ϕ_1, ϕ_2 respectively, we use (54),(55) to calculate the $2n$ vector estimates

$$\theta_{1i} = (B^*(\phi_1)) \in \mathbf{R}^9 \text{ and } \theta_{2i} = (B^*(\phi_2)) \in \mathbf{R}^9; i = 1, 2, \dots, n \quad (56)$$

If Part I of the conjecture holds, or if we have other information stating that we have approximate Gaussian distributions in $DIFFEO(X)$ it follows that the linear estimates in (56) also have approximate Gaussian distributions. Then we can apply Hotelling's T^2 test and in the present situation the test statistic reduces to the following procedure.

Compute the empirical mean value vector difference

$$\bar{\theta}_1 = \frac{1}{n_1} \sum_{i=k}^{n_1} \theta_{1k}; \bar{\theta}_2 = \frac{1}{n_2} \sum_{k=1}^{n_2} \theta_{2k} \quad (57)$$

and the empirical covariance matrix Σ

$$\Sigma = \frac{1}{n_1 + n_2 - 2} \left\{ \sum_{k=1}^{n_1} [\theta_{1k} - \bar{\theta}_1][\theta_{1k} - \bar{\theta}_1]^T + \sum_{k=1}^{n_2} [\theta_{2k} - \bar{\theta}_2][\theta_{2k} - \bar{\theta}_2]^T \right\} \quad (58)$$

Then the statistic

$$T^2 = \frac{n_1 n_2}{n_1 + n_2 - 2} (\theta_1 - \theta_2)^T \Sigma^{-1} (\theta_1 - \theta_2) \quad (59)$$

can be used to construct a test with the critical region

$$T^2 > \frac{9(n_1 + n_2 - 2)}{n_1 + n_2 - 10} F_{9, n_1 + n_2 - 10}(p) \tag{60}$$

on the significance level p ; see Anderson (1958). In parenthesis we mention that this test has the advantage of being affine invariant.

So far, so good. But we are not likely to have sample sizes so big that $n_1 + n_2 > 10$, which is needed for the above to be valid. A way out of this dilemma is to reduce the dimensionality of the θ -vectors from 9 to some lower value d and apply the test to the new samples with reduced dimensionality. For example, compute the principal components of the θ samples and use the d most important. One such procedure has been given in Langsrud (2002).

It will be of value to find the properties of the leading principal components. For example the first one: is it approximately a symmetric function (like the sum or product) of the λ 's in Section 3?

One could use other functionals than the θ 's to reduce the dimensionality, for example based on an orthonormal function system tailored to the α set. We should mention Antoniadis (2003) who employs wavelets to execute the FANOVA. We also refer to an important paper Cao, Worsley (1999) that studies shape changes in terms of the Euler characteristic, rather than group properties, and applies the method to brain data.

10 Putting it all together

. We are therefore faced with the following stages of MICKEY:

- (1) The data collection phase, when MRI's are collected for knockout as well as for normal mice.
- (2) Computation of the diffeomorphisms making sure that no spurious effects are introduced.
- (3) Development of biologically meaningful mathematical models of growth.
- (4) Introduction of a set of statistics extracted from the computed diffeomorphisms.
- (5) Data analysis based on these statistics.
- (6) Testing hypothesis about the influence of gene manipulations on the observed growth.

11 REFERENCES

.
 U. Grenander, M.I. Miller and J. Zhang(2003): FANOVA of genetically modified mouse brains, Div. Appl. Math, Brown University, Rep. No. 3

- F. Bookstein (1978): The measurement of biological shape and shape changes, Lecture Notes in Biomathematics 24, Springer-Verlag
- U.Grenander, M.I.Miller (1998) Computational anatomy, Quarterly of Appl. Math., LVI Bonner, J.T., ed. 1982: Evolution and Development. Report of the Dahlem Workshop on Evolution and Development, Berlin 1981. Berlin/New York: Springer Verlag.
- D. G. Kendall, D. Barden T. K. Carne, H. Lee(1999): Shape and Shape Theory, Wiley Series in Probability and Statistics
- O. Langsrud (2002): 50-50 Multivariate Analysis of Variance for Collinear Responses, The Statistician, 51
- R.A. Vitale (1974): Convolutions on a group arising in pattern analysis, Ph. D. Thesis, Brown University
- J.Cao, K.J. Worsley (1999): The detection of local shape changes via the geometry of Hotelling's T² fields. Annals of Statistics, 27
- G.E. Christiansen (1994): Deformable shape models for anatomy, Ph. D. Thesis, Washington University
- L. Matejic (1997): Group cascades for representing biological variability, Ph.D. Thesis, Brown University
- M. F. Beg, M. I. Miller, A. Trouve, L. Younes (2002): Computing Metrics on Anatomical Shapes in Computational Anatomy. Second Joint Meeting of IEEE EMBS-BMES Society
- D.Mumford (2002): Pattern Theory: The Mathematics of Perception. APPTS Report No. 02-10, Div. Appl. Math., Brown University
- P.M. Thompson, A.W. Toga(2002): A Framework for Computational Anatomy, Computing and Visualization in Science
- A.Antoniadis(2003): Optimal Testing in Functional Analysis Models, University of Florida, Department of Statistics, Fifth Annual Winter Workshop
- T.W. Anderson (1958): An introduction to multivariate statistical analysis, Wiley